Granular Matter (2007) 9:241–250
DOI 10.1007/s10035-007-0037-3

Influence of pile shape and pile interaction on the crushable behavior of granular materials around driven piles: DEM analyses

Sebastian Lobo-Guerrero · Luis E. Vallejo

Received: 22 November 2005 / Published online: 23 March 2007

Abstract This study presents an analysis and a visualization of the effect that the pile shape has on the penetration resistance of driven piles in crushable granular materials. Discrete Element Method (DEM) simulations of single piles with different shapes (flat tip, open pile, triangular tip) being driven into a previously compacted uniform crushable soil are presented. The results from the DEM simulations showed that the shape of the driven piles has a significant influence on the development of penetration resistance and particle crushing. This study also presents the penetration resistance and particle crushing results when a second flat tip pile was driven in a region near a pre-existing single flat tip pile. It was found that considerable high crushing was induced by the second pile. The second pile induced crushing not only on the particles surrounding itself but also on the particles surrounding the pre-existing pile, showing that particle crushing around a driven pile not only takes place when the pre-existing pile is being driven, but it also occurs during the installation of a second pile, in a region closely located to the first one.

Keywords Particle crushing · Penetration resistance · Driven piles · Pile shape · Pile interaction

S. Lobo-Guerrero
Geotechnical Project Specialist, American Geotechnical and Environmental Services, Inc., Canonsburg, PA 15317, USA
e-mail: sebastianl@agesinc.com

L. E. Vallejo (✉)
Department of Civil and Environmental Engineering, University of Pittsburgh, 949 Benedum Hall, Pittsburgh, PA 15261, USA
e-mail: vallejo@civ.pitt.edu

1 Introduction

The analysis and design of pile foundations on crushable soils such as carbonate sands or weathered volcanic soils is complicated by their high compressibility and highly curved Mohr–Coloumb failure envelopes [21]. When a pile is driven into a weak granular material, stresses concentrate around its tip causing the breakage of some particles. This breakage causes a reduction in volume of the material surrounding the pile due to the rearrangement of the unbroken particles and the produced fragments, and the migration of fine particles through the pore spaces of the unbroken grains. This process continues as the pile is driven further down leading to a stress relaxation on the granular material located around the pile [7,17,19,20]. Thus, it is widely accepted that the capacity of driven piles in breakable weak sands is only a fraction of the capacity of driven piles in strong sands such as quartz sands [1,8,15]. The objective of this study is to present an analysis and a visualization of the effect that the pile shape has on the penetration resistance of driven piles in crushable granular materials. The interaction between two driven piles is also studied, investigating the effect of particle crushing on the behavior of pile groups. This study is an extension to that presented by [12] in which grain crushing due to a single driven pile with a triangular tip was analyzed.

2 Previous work on particle crushing

Previous researchers have used centrifuge tests and calibration chamber tests on carbonate (calcareous) sands to understand what really occurs when driving a pile

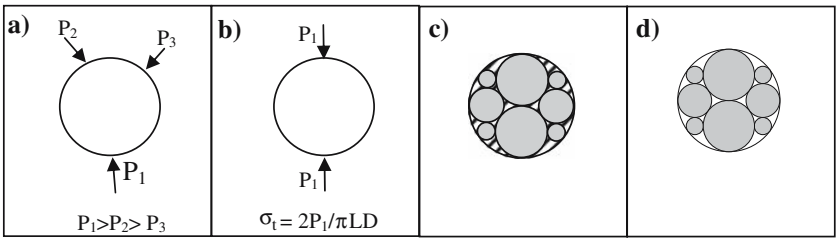

Fig. 1 Idealization of the induced tensile stress and arrangement of the produced fragments

into a weak sand [14,19,20]. Particle crushing has been identified as a phenomenon that negatively affects the capacity of driven piles. Some techniques such as X-ray CT (Computed Tomography) scanning are also being used to study particle crushing and its evolution around driven piles [16].

Previous research has shown that numerical simulations in the form of the Discrete Element Method (DEM) can be used for the visualization of crushing in granular materials. Since the original DEM developed by [6] did not consider particle breakage, different solutions have been proposed in order to overcome this constraint. Some of these solutions include the consideration of each granular particle as an agglomerate of bonded smaller particles that can later disaggregate, and the replacement of particles fulfilling a predefined failure criterion with a group of smaller particles [2,3,10, 18]. This study uses the second solution and a simplified failure criterion to simulate the evolution of crushing around driven piles.

3 Particle breakage criterion

The PFC^{2D} program which is based on DEM was used. When using this program, particles are idealized as discs that interact with each other at their contacts. This interaction is mainly governed by two models: the stiffness model and the slip model (Itasca, Theory and Background [9]). Since the PFC^{2D} program does not allow particle breakage, a subroutine using the FISH language (Itasca, FISH in PFC 2002) was programmed based on a failure criterion previously developed by the authors [11–13]. In these publications the authors analyzed the crushing behavior of granular material under different conditions of stress and strain such as in a direct shear test, different stress paths on biaxial compression, and around a single pile of fixed shape driven into a granular material. The present study extends the previous work to include the effect of pile shape and the number of piles on the crushing behavior of granular materials. The details and background of the adopted model have been presented in the cited references. The main assumptions of the model are summarized:

- Only particles with a coordination number equal to or smaller than 3 are able to be broken.
- For those particles having a coordination number smaller than or equal to 3, the loading configuration such as the one presented in Fig. 1a is assumed to be equivalent to a Brazilian test, as shown in Fig. 1b. The induced tensile stress, σ_t, can be obtained with the expression presented on Fig. 1b, where P_1 is the value of the highest contact force acting on the particle, L is the thickness of the disk (unit thickness for the simulated case), and D is the diameter of the disk.
- The tensile strength of a particle having a radius of 1 mm is predefined as $\sigma_{\max 1\,\mathrm{mm}} = 3 \times 10^6$ Pa, and is assumed that the tensile strength of a particle with a radius r, $\sigma_{\max}(r)$, is related to $\sigma_{\max 1\,\mathrm{mm}}$ according to the following relationship (where r is expressed in mm/mm since it needs to be normalized by the standard value of 1 mm): $\sigma_{\max}(r) = \sigma_{\max 1\,\mathrm{mm}}[r]^{-1}$.
- Every particle with a coordination number smaller than or equal to 3 is allowed to break if $\sigma_t > \sigma_{\max}(r)$.

Every particle fulfilling the failure criterion breaks into the eight fragments shown on Fig. 1c, and many fine particles represented by the dashed area in this figure. However, the finer particles will migrate through the pore spaces between the surrounding particles, and for the sake of computer efficiency this material is not considered in the model (Fig. 1d). The properties of the new fragments are similar to those of the breaking particle. The subroutine does not restrict smaller particles from continuing to break. Thus, different generations of crushing coexist inside the simulated granular material.

4 Configuration of the simulated crushable soil and simulated piles

A virtual container having a width of 40 cm and a height of 80 cm was constructed. The shear and normal

stiffnesses of the walls forming the box were set to 1×10^9 N/m. The walls were assumed to have a friction coefficient of 0.7. The original granular material was simulated by 6,500 discs with a radius of 3 mm. The density of the discs was set to 2,500 kg/m^3, their normal and shear stiffnesses were set to 1×10^8 N/m, and their friction coefficient was set to 0.7. The 6,500 particles were generated inside the virtual container (avoiding overlaps between particles) and were allowed to settle down due to the gravity forces ($g = 9.8$ m/s^2). Compaction of the sample was induced by moving the top horizontal wall of the box downwards until the forces generated inside the sample were approaching the values required to induce particle crushing. After unloading, the top wall was deleted. The friction coefficient of the particles and walls were temporarily set to zero during the compaction process. After compaction, three copies of the simulation were recorded since they were the start of the simulations considering different single piles.

The simulated single piles had three different shapes: a flat closed tip, an open end, and a triangular closed tip (two inclined planes forming 45° with the vertical). The piles having a flat closed tip and a triangular closed tip had a constant pile width of 3 cm. The open pile had an internal width of 3 cm and a wall thickness of 1 mm. The friction coefficients of the piles were set to a value of 0.7, and their coefficients of normal and shear stiffness were set to 1×10^9 N/m. The single piles were driven at a vertical velocity of 1×10^{-6} m/step up to a penetration depth of 45 cm (15 times the width of the piles). The ratio of pile width to the particle diameter was equal to 5. This may have had an effect on the results since is considerably smaller than the values between 10 and 20 suggested by other researchers for the accurate prediction of the load that a pile can resist [4]. In order to increase this ratio to a value of at least 10 and maintain a considerable distance between the pile and the lateral and lower boundaries of the domain, the initial number of particles would have to increase from 6,500 to about 26,000. Also, this new number of particles will increase as a result of crushing (increasing the run time of the simulations). For the sake of computer efficiency, the authors considered as a reasonable alternative to use a ratio of pile diameter to particle size equal to 5.

After the single pile with the flat tip was driven to a depth of 45 cm (15 times its diameter), a second pile was driven near to it to investigate the effect of pile interference. The horizontal distance between the centers of the piles was equal to three times the diameter of the piles. The properties of the second pile were equal to those used on the first pile. Also, the driving velocity was equal to the one used to install the first pile.

5 Results of the tests considering single piles of different shapes

Figure 2 show some snapshot of the virtual single piles being driven through the same initial material. The figures focus on the piles and the surrounding particles and do not show the whole extent of the simulated samples. The fragments produced as a result of crushing are shown as dark particles. The dark regions on the snapshots correspond with regions where crushing took place. Considerable stresses were induced ahead of the tips of the piles, generating crushing of the material in these zones. After the tips of the piles passed through the zones where crushing took place, the fragments coated the shafts of the simulated piles. For the open pile, a considerable amount of crushed particles went inside the shaft. Figure 3 shows amplified details of the piles at a penetration depth of 45 cm. The color of each particle in this figure indicates the generation of crushing that the particle represents. A maximum of a fifth generation of crushing was produced during the simulation of

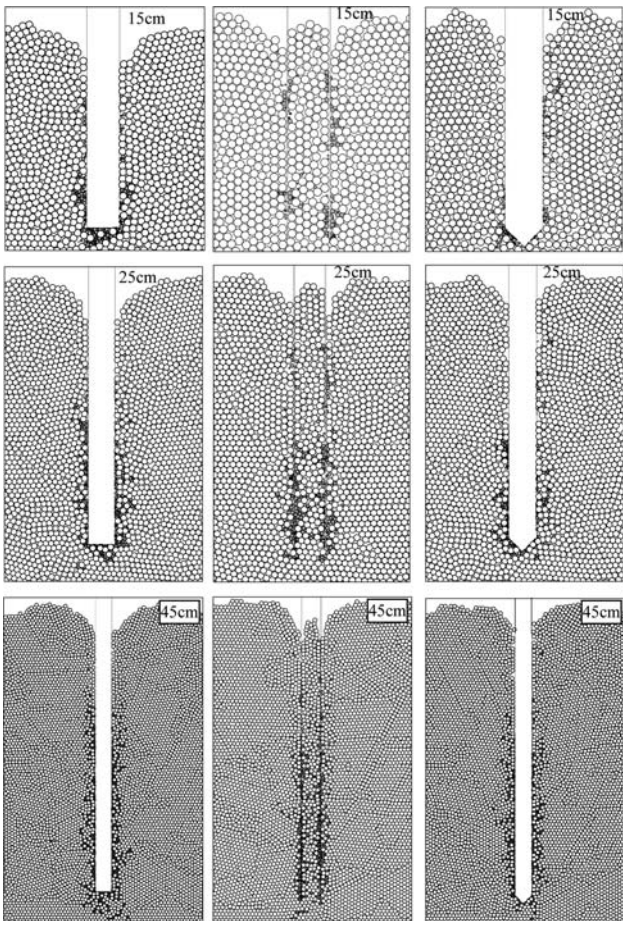

Fig. 2 Snapshots of the simulated single piles at different penetration depths

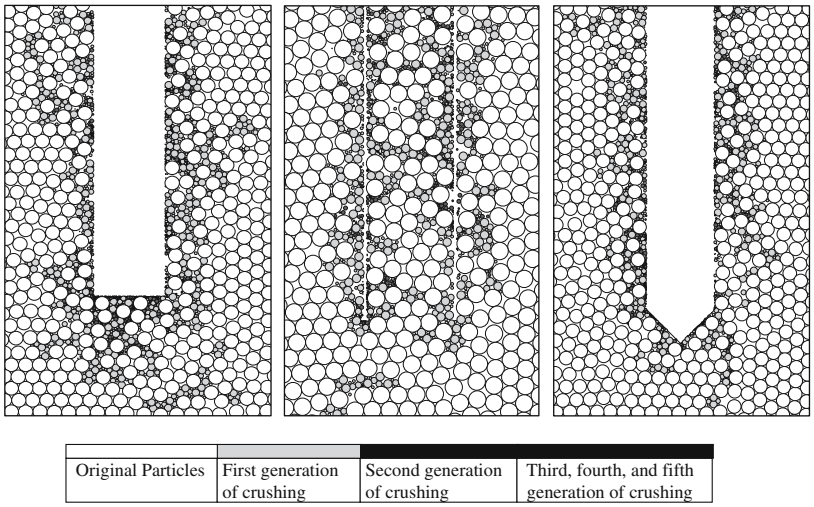

Fig. 3 Amplified details of the particles around the piles at a penetration depth of 45 cm (15× width of the piles)

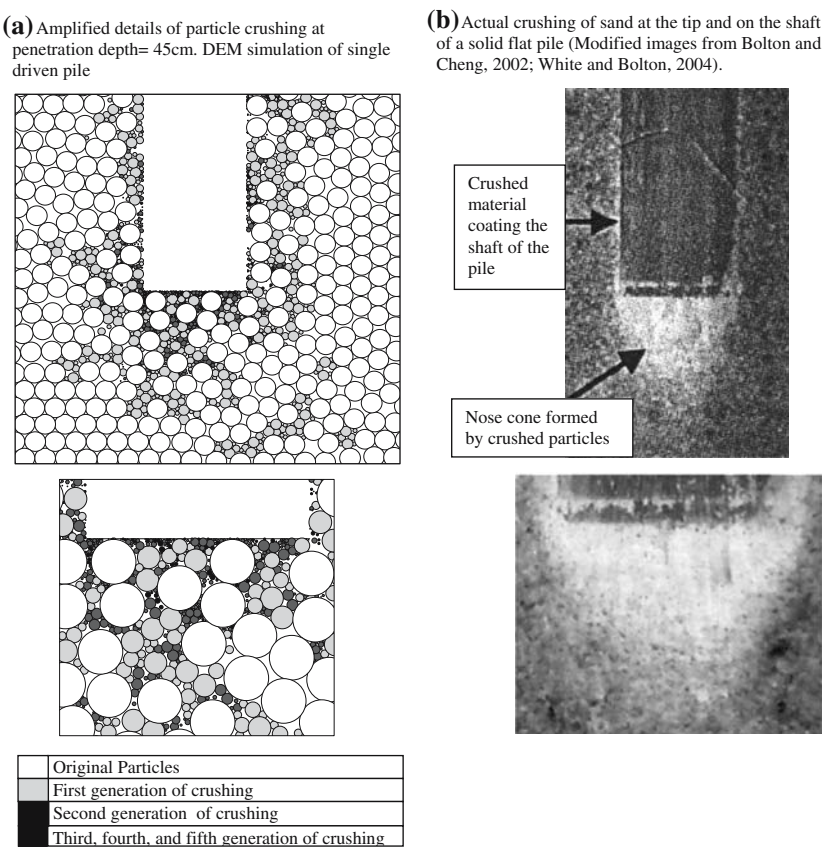

Fig. 4 Amplified details: **a** DEM simulation of the single pile with flat tip, **b** Real pile with flat tip

the pile with the closed flat tip while a maximum of a fourth generation of crushing was produced during the simulations of the other two piles. More crushing was produced underneath the tip of the flat ended pile than underneath the other two piles.

Figure 4 shows a comparison between the snap shots of the DEM simulation considering the single pile with flat tip at a penetration depth of 45 cm and some pictures of a real small pile driven in sand. The pile tests were conducted in a plane strain calibration chamber [5,20]. The DEM snap shots and the photos of the pile test on the calibration chamber show that particle crushing took place underneath the flat tip creating a nose cone. After the tip of the piles passed through the crushed material, the generated fragments coated the shaft of the pile. The good agreement between the predicted behavior using

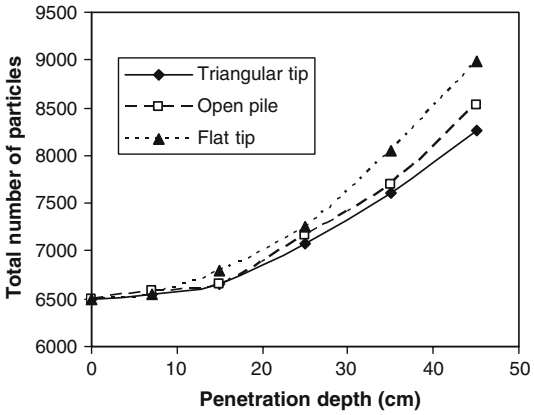

Fig. 5 Total number of particles after crushing at different penetration depths, single piles

the DEM simulation and the results obtained in the actual pile test validates the use of the particle breakage model used in this study.

In order to compare the amounts of crushing produced during the DEM simulations, the total number of particles at different stages was calculated. These results are presented in Fig. 5, showing that more crushing was produced during the simulation of the pile with the flat tip. Also, more crushing was produced during the simulation of the open pile than during the simulation of the pile with the triangular tip. This is because a plug developed inside the open pile, converting this pile into a kind of closed flat ended pile. The open pile was then driven in a semi-plugged mode since the plug was still able to deform and slip inside the shaft. The real rigid flat tip produced more crushing than the annulus and deformable plug system of the open pile. Figure 6 shows snapshots of the forces developed around the tip of the pile with the flat closed tip and around the open pile. For the pile with the flat tip, the forces concentrated underneath the tip and were transmitted directly to the rigid horizontal wall. For the open pile, the forces concentrated underneath the tip and were transmitted to the internal shaft of the pile in a short distance from the tip.

The resistant forces developed at the shafts and tips of the piles were measured during the tests. Figure 7 shows the total force developed at the tip and at the shaft of the pile with the flat tip at different penetration depths. The resistance to penetration curves showed spike drops as a result of particle crushing and particle rearrangement. This trend was also observed on the results of the other two single piles. Table 1 shows the results at a penetration depth of 45 cm for the three single piles (the showed values are the average values measured during the final part of the simulations). The pile with the flat closed tip developed the highest total penetration resistance, followed by the open pile and the pile with the triangular tip. This is the exact same order of the amount of produced crushing. The pile with the triangular tip seems to produce the lowest amount of crushing and the lowest value of total penetration resistance while the flat ended pile develops higher values of penetration resistance inducing important amounts of crushing.

6 Effect of pile interference

As mentioned before, after the single pile with the flat tip was driven to a depth of 45 cm, a second pile was driven near to it to investigate the effect of pile interference. Figure 8 shows the resistance to penetration curves for the shaft and tip of the second pile, and some snap shots at different penetration depths. The inclusion of the first pile caused the heave of the ground level. The second pile had to be driven 52.4 cm (17.5 times the diameter of the pile) in order to reach the elevation of the tip of the first pile. Average values of 8×10^4 N and 2.5×10^4 N

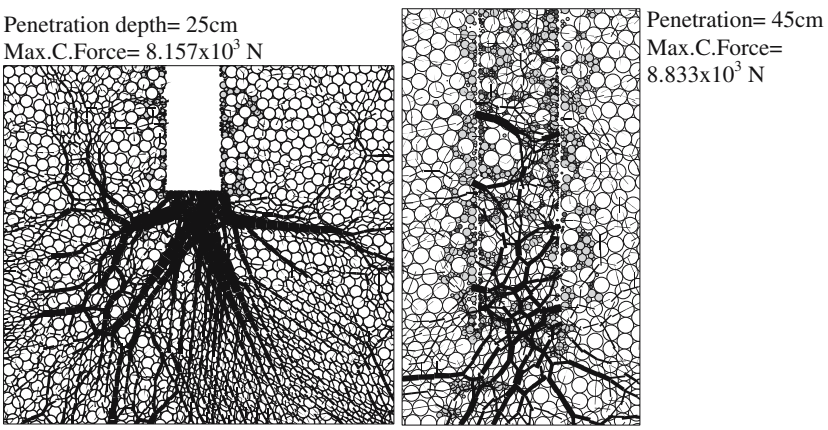

Fig. 6 Examples of the forces developed around the tips of a solid flat-tip pile and a hollow pile

Table 1 Resistant vertical forces at a penetration depth of 45 cm (15× width of the piles)

Pile type	Total vertical force at pile tip (N)	Total vertical force at external shaft (N)	Total vertical force at internal shaft (N)	Total vertical resistance (N)
Flat closed tip	4.5×10^4	0.75×10^4	–	5.25×10^4
Open pile	0.8×10^4	1×10^4	1.9×10^4	3.7×10^4
Triangular tip	2.9×10^4	0.6×10^4	–	3.5×10^4

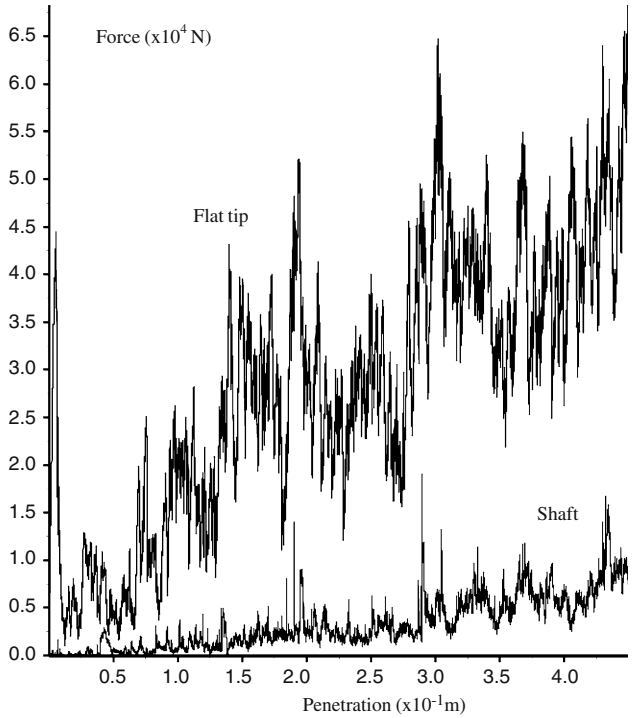

Fig. 7 Resistant forces on a single pile with flat tip at different penetration depths

were recorded at the end of the simulation for the tip and shaft resistance, respectively. The tip resistance for the second pile was 1.78 times the tip resistance generated by the first pile. The shaft resistance for the second pile was 3.33 times the shaft resistance generated by the first pile. The increment on the penetration resistance seems to be the effect of a densification of the soil caused by the installation of the first pile.

The snap shots in Fig. 8 show that crushing originated underneath the tip of the second pile, and as the pile continued to penetrate, the crushed material coated its shaft. Figure 9 shows some amplified details at penetration depth of 52.4 cm. This figure shows that considerably more crushing was induced by the second pile than the first pile although no more than a fifth generation of crushing was produced during the simulation. Moreover, a comparison between Figs. 9 and 3 and Fig. 4a shows that the installation of the second pile induced the breakage of some particles around the first pile. The force chains generated by the installation of the second pile can be used to explain this phenomenon. Figure 10 shows an example of these force chains at a penetration depth of 35 cm. As shown in this figure, the force chains spread principally from the tip of the pile in different directions. Some of the force chains reached the first pile and the material surrounding it. Thus, particle crushing was induced on some particles located near the first pile.

Figure 11 shows the velocity vectors of the particles located near to the piles at the end of the test. As shown on this figure, the particles located underneath the tip of the second pile moved vertically and laterally towards the first pile. More surprisingly, particles located underneath the first pile moved laterally due to the forces induced by the installation of the first pile (as shown in Fig. 10). Some movement also took place around the shafts of both piles, but it concentrated around the shaft of the second pile. The results presented from Fig. 8 through Fig. 11 evidenced the fact that particle crushing and particle rearrangement took place near the first pile due to the installation of the second pile.

Figure 12 shows the total number of particles during different stages of the simulation. The data regarding the crushing produced by the installation of the first pile (reported on Fig. 5) was included in this figure for comparison. The total number of particles at a penetration depth of 45 cm for the first pile is the same number of particles at a penetration depth of 0 cm for the second pile since this stage represents the starting of the second test. It can be seen that significantly more crushing was produced during the installation of the second pile than during the installation of the first pile. The DEM results also show that the penetration resistance of the second pile was higher than the one recorded for the first pile. This increase in penetration resistance in the second pile is the result of: (a) densification of the zones around the preexisting pile as a result of its installation, and (b) the crushed particles resulting from the installation of the first pile. These crushed particles also crush during the installation of the second pile. Since these original crushed particles need a higher stress to further crush them,

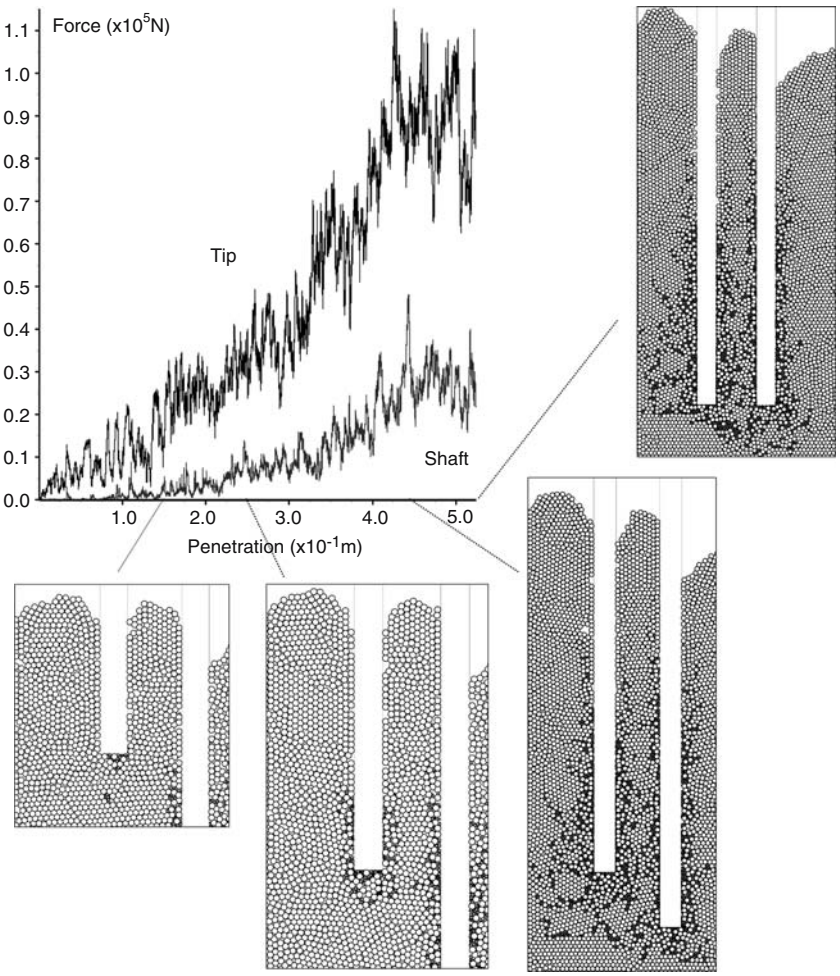

Fig. 8 Resistant forces on the second pile with flat tip at different penetration depths

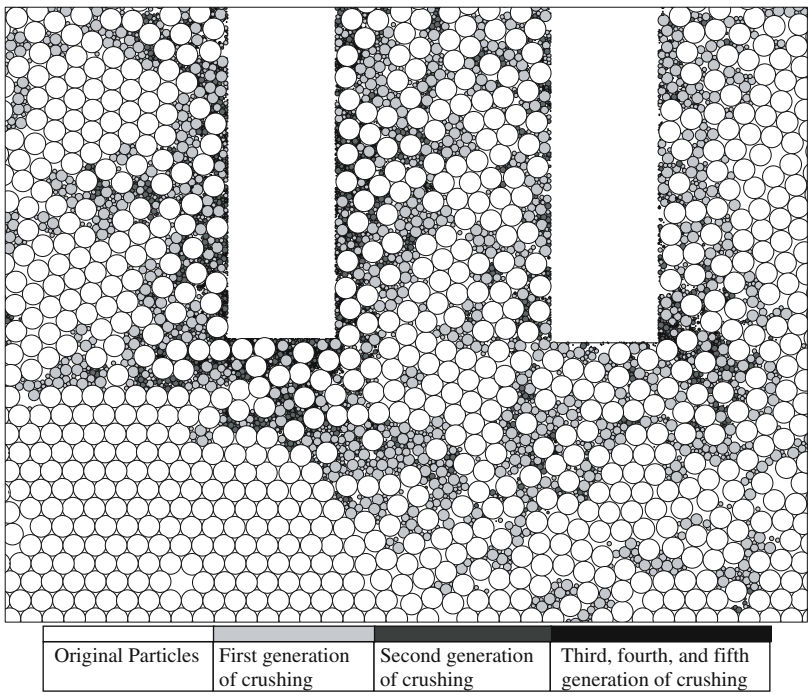

Fig. 9 Amplified details of the particles around the second pile at a penetration depth of 52.4 cm (17.5 times the pile diameter)

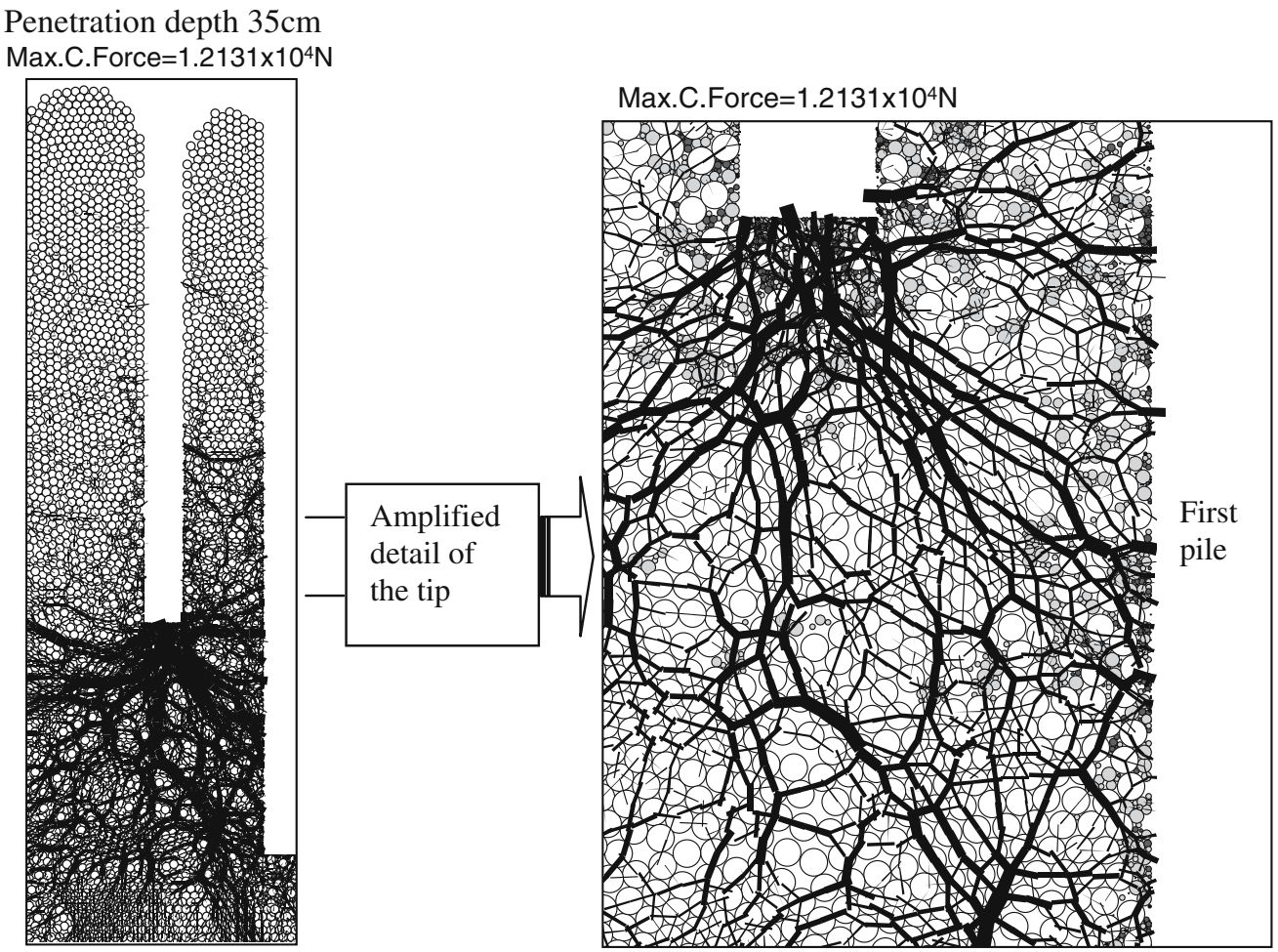

Fig. 10 Example of the force chains generated during the installation of the second pile

this increase in crushing stress is reflected in the higher value of penetration resistance measured for the second pile.

The obtained results show that particle crushing around a driven pile not only occurs when one pile is being driven, but it also takes place during the installation of a second pile located near the preexisting one. Moreover, a higher amount of crushing is generated during the installation of the second pile compared to the amount generated during the installation of the first pile. Also, the penetration resistance is higher during the installation of the second pile as is the amount of particles that crush. Previous published results have focused on crushing of granular materials during the installation of a single pile. The authors are not aware of any experimental results addressing particle crushing around pile groups. Thus, the findings obtained in this study need experimental validation before drawing more definitive conclusions.

7 Limitations of the simulations

The obtained results need to be treated with some caution since they were developed in order to provide a general visualization and a better understanding of the evolution of crushing around driven piles. In particular they were developed to study the influence of pile shape and the interaction between driven piles on crushable granular materials. Many simplifications such as considering a two dimensional space, and the representation of the granular material with a group of dry circular particles, needed to be done due to the adopted numerical technique. Moreover, due to computational efficiency the ratio between pile diameter and particle diameter was some how low. The adopted particle breakage model did not consider particle abrasion although this kind of particle degradation was less likely to occur on circular particles. All these assumptions could affect the exact numerical values obtained during the simulations. Nev-

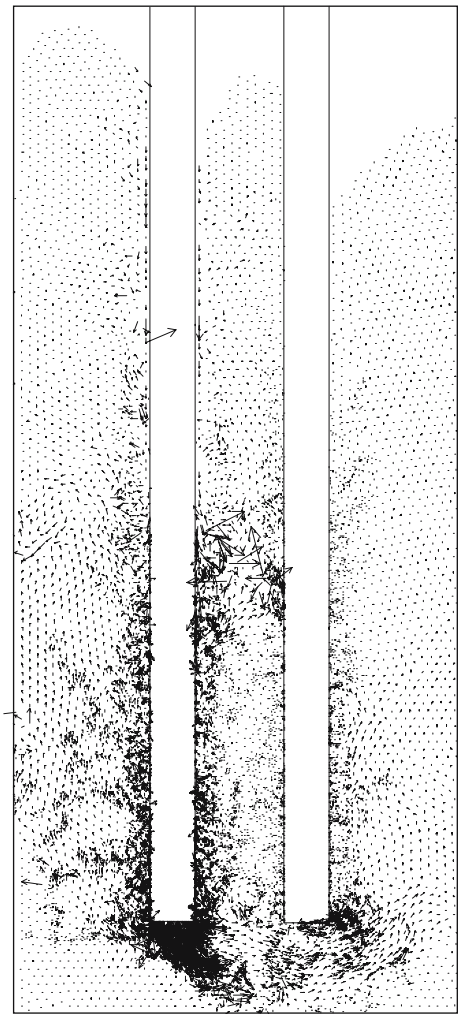

Fig. 11 Velocity vectors of the particles around the second pile at a depth of penetration equal to 52.4 cm

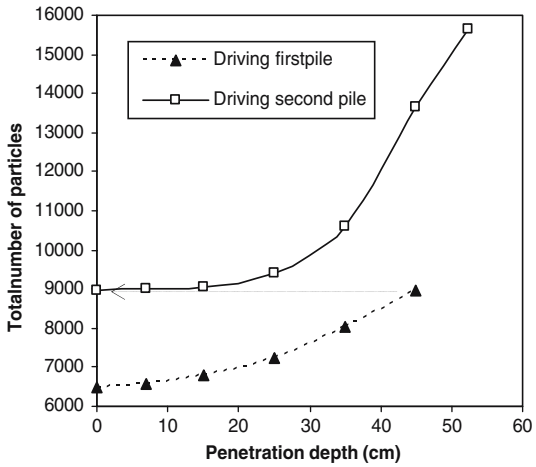

Fig. 12 Total number of particles after crushing at different penetration depths, two driven piles

ertheless, regardless of all these assumptions, some of the obtained results agree with experimental evidence such as the case presented on Fig. 4 and field behavior reported on the literature. On the other hand, at this moment there is not published experimental evidence that can be used to asses the validity of other results such as the evolution of particle crushing in pile groups. Consequently, future experimental research is needed to validate the behavior predicted by some of the simulations.

8 Conclusions

The results from the DEM simulations showed that the shape of the driven pile has a significant influence on the development of penetration resistance and particle crushing. The highest penetration resistance was recorded on a flat ended pile as compared to that obtained on an open pile or on a pile with triangular tip. The flat ended pile also induced the highest amount of crushing on circular particles surrounding it. The pile with the triangular tip presented the lowest value of penetration resistance and produced the least amount of crushing. The open (hollow) pile developed an inside plug during the driving process and at the end of the test it was found to be operating in a semi-plugged mode. The lower part of the open pile tended to behave as a flat closed tip because of the plug, but this plug was not rigid, allowing internal deformations and slipping relative to the internal shaft. However, it should be noted that the formation of the plug will depend upon the boundary conditions of the open pile (i.e., the ratio between the diameter of the interior of the pile and the size of the particles, as well as on the frictional characteristics of the interior of the pile and those of the granular material).

The simulation considering the installation of two piles (separated by a distance equal to three times their diameter) showed that particle crushing around a driven pile not only occurs when the first pile is being driven, but it also takes place in areas around the first pile as a result of the installation of the second pile. The installation of the first pile causes a densification of the granular material, this in turn causes an increase in penetration resistance of the second pile and produces considerably more crushing than the one caused during the installation of the first pile. However, it should be noted that the analysis presented is a 2D analysis. The interaction between two piles will be different in two dimensions than in three dimensions: a second pile in 2D experiences different boundary conditions than those in a 3D case. Nevertheless, the 2D analysis helps in the visuali-

zation and understanding of the pile(s)-soil interaction problem.

Acknowledgements This work was supported by Grant No. CMS-0301815 to the University of Pittsburgh from the National Science Foundation, Washington, D.C. This support is gratefully acknowledged.

References

1. Al-Douri, R.H., Poulos, H.G.: Static and cyclic direct shear tests on carbonate sands. Geotech. Testing J. **15**(2), 138–157 (1991)
2. Astrom, J.A., Herrmann, H.J.: Fragmentation of grains in a two-dimensional packing. Euro. Phys. J. B **5**, 551–554 (1998)
3. Astrom, J.A., Herrmann, H.J., Timonen, J.: Fragmentation dynamics within shear bands—a model for aging tectonic faults?. Euro. Phys. J. E **4**, 273–279 (2001)
4. Bolton, M.D., Gui, M.W., Garnier, J., Corte, J.F., Bagge, G., Laue, J., Renzi, R.: Centrifuge cone penetration tests in sand. Geotechnique **49**(4), 543–552 (1999)
5. Bolton, M.D., Cheng, Y.P.: Micro-geomechanics. In: Springman, S.M. (ed.) Constitutive and Centrifuge Modelling: Two Extremes, pp 59–71. Swets & Zeitlinger, Lisse (2002)
6. Cundall, P.A., Strack, O.D.L.: A discrete numerical model for granular assemblies. Geotechnique **29**(1), 47–65 (1979)
7. DeJong, J.T., Randolph, M.F., White, D.J.: Interface load transfer degradation during cyclic loading: a microscale investigation. Soils Found. **43**(4), 81–93 (2003)
8. Gilchrist, J.M.: Load tests on tubular piles in coralline strata. ASCE J. Geotech. Eng. **111**(5), 641–655 (1985)
9. Itasca Consulting Group, Inc. (2002). PFC^{2D} (Particle Flow Code in Two Dimensions) version 3.0; sections: Theory and Background; FISH in PFC
10. Jensen, R.P., Plesha, M.E., Edil, T.B., Bosscher, P.J., Kahla, N.B.: DEM simulation of particle damage in granular media—structure interfaces. Int. J. Geomech. **1**(1), 21–39 (2001)
11. Lobo-Guerrero, S., Vallejo, L.E.: Analysis of crushing of granular material under isotropic and biaxial stress conditions. Soils Found. **45**(4), 79–87 (2005)
12. Lobo-Guerrero, S., Vallejo, L.E.: DEM analysis of crushing around driven piles in granular materials. Geotechnique **55**(8), 617–623 (2005)
13. Lobo-Guerrero, S., Vallejo, L.E.: Discrete element method evaluation of granular crushing under direct shear test conditions. ASCE J. Geotech. Geoenviron. Eng. **131**(10), 1295–1300 (2005)
14. McDowell, G.R., Bolton, M.D.: Effect of particle size distribution on pile tip resistance in calcareous sand in the geotechnical centrifuge. Granular Matter **2**, 179–187 (2000)
15. Murff, J.D.: Pile capacity in calcareous sands: state of the art. ASCE J. Geotech. Eng. **113**(5), 490–507 (1987)
16. Otani, J., Mukunoki, T., Sugawara, K.: Evaluation of particle crushing in soils using x-ray CT data. Soils Found. **45**(1), 99–108 (2005)
17. Randolph, M.F.: Science and empiricism in pile foundation design. Geotechnique **53**(10), 847–875 (2003)
18. Tsoungui, O., Vallet, D., Charmet, J.C.: Numerical model of crushing of grains inside two-dimensional granular materials. Powder Technol. **105**, 190–198 (1999)
19. White, D.J., Bolton, M.D.: Observing friction fatigue on a jacked pile. In: Springman, S.M. (ed.) Centrifuge and Constitutive Modelling: Two Extremes, pp 347–354. Balkema, Rotterdam (2002)
20. White, D.J., Bolton, M.D.: Displacement and strain paths during plane-strain model pile installation in sand. Geotechnique **54**(6), 375–397 (2004)
21. Yasufuku, N., Hyde, A.F.L.: Pile end-bearing capacity in crushable sands. Geotechnique **45**(4), 663–676 (1995)